

A Numerical Study of Cirrus Clouds. Part I: Model Description

HUI-CHUN LIU, PAO K. WANG, AND ROBERT E. SCHLESINGER

Department of Atmospheric and Oceanic Sciences, University of Wisconsin—Madison, Madison, Wisconsin

(Manuscript received 2 November 2000, in final form 7 November 2002)

ABSTRACT

This article, the first of a two-part series, presents a detailed description of a two-dimensional numerical cloud model directed toward elucidating the physical processes governing the evolution of cirrus clouds. The two primary scientific purposes of this work are (a) to determine the evolution and maintenance mechanisms of cirrus clouds and try to explain why some cirrus can persist for a long time; and (b) to investigate the influence of certain physical factors such as radiation, ice crystal habit, latent heat, ventilation effects, and aggregation mechanisms on the evolution of cirrus. The second part will discuss sets of model experiments that were run to address objectives (a) and (b), respectively.

As set forth in this paper, the aforementioned two-dimensional numerical model, which comprises the research tool for this study, is organized into three modules that embody dynamics, microphysics, and radiation. The dynamic module develops a set of equations to describe shallow moist convection, also parameterizing turbulence by using a 1.5-order closure scheme. The microphysical module uses a double-moment scheme to simulate the evolution of the size distribution of ice particles. Heterogeneous and homogeneous nucleation of haze particles are included, along with other ice crystal processes such as diffusional growth, sedimentation, and aggregation. The radiation module uses a two-stream radiative transfer scheme to determine the radiative fluxes and heating rates, while the cloud optical properties are determined by the modified anomalous diffraction theory (MADT) for ice particles. One of the main advantages of this cirrus model is its explicit formulation of the microphysical and radiative properties as functions of ice crystal habit.

1. Introduction

It has recently become clear that cirrus clouds significantly affect the global energy balance and climate, due to their great radiative impact on atmospheric thermal structure. Randall et al. (1989) used a general circulation model (GCM) to perform simulations and showed that upper-tropospheric clouds have dramatic impacts on the large-scale circulation in the Tropics with attendant effects on precipitation and water vapor amounts. Ramaswamy and Ramanathan (1989), also through GCM studies, suggested that the discrepancies between the simulated and observed upper-tropospheric temperature structure in the Tropics and subtropics can be explained by the radiative heating effects of cirrus cloud systems. These studies point out that cirrus clouds are likely to have great impacts on the radiation and hence the intensity of the general circulation. They also indicated that the impact of the quality of parameterizations related to cirrus clouds on the results of the GCM may be significant. Other studies had also shown that variations in the assumed cirrus radiative properties can

significantly alter the results of climate models (Ramanathan et al. 1983; Liou 1992).

The radiative properties of cirrus depend on their microphysical properties such as ice crystal habit, ice water content, and number concentration. The microphysical properties, in turn, are determined by the atmospheric forcing and environmental conditions such as large-scale lifting, static stability, temperature, and moisture. For example, one possible scenario of cirrus development could be that the cloud forms during the lifting of moist air associated with large-scale motions, as small ice crystals are formed in the embedded updraft. If the upward motion persists long enough to cause further cooling of the layer, ice crystals will precipitate by growing to sizes with substantial fall velocities. As cirrus cloud evolves, the corresponding in-cloud radiative heating patterns change accordingly. The resulting radiative heating profile changes the temperature lapse rate and, thus, the cloud dynamics. A change in cloud dynamics resulting from the vertical velocity variations due to changes in temperature lapse rate may, for example, modify the ice saturation ratio and thus the growth rate of ice, which in turn affects the microphysical processes to alter the size distribution of ice crystals, further modifying the radiative heating profiles within the cloud. Therefore, the feedback mechanisms among cirrus radiative properties, microphysical prop-

Corresponding author address: Dr. Pao K. Wang, Dept. of Atmospheric and Oceanic Sciences, University of Wisconsin—Madison, 1225 W. Dayton Street, Madison, WI 53706-1695.
E-mail: pao@windy.aos.wisc.edu

erties, and atmospheric condition are rather complex, making the parameterizations of these feedback mechanisms a difficult task.

It is known that parameterizations for describing cirrus cloud properties are often highly simplified (Del Genio et al. 1996). In simulating climate, these schemes are simple partly because of the coarse spatial and temporal resolution in global circulation models, and partly due to our poor understanding of the microphysical properties of cirrus and how cirrus responds to changes in environmental conditions. In some GCMs, it is assumed that cirrus clouds occur when the resolvable-scale relative humidity exceeds some critical values. More sophisticated GCMs represent cirrus clouds either by diagnosing the ice water content from the predicted total water content as a function of temperature (Del Genio et al. 1996) or by using a prognostic formulation to predicting cloud ice mixing ratio (Fowler et al. 1996). All of these schemes, however, do not allow supersaturation with respect to ice in the model, and this may overestimate the growth rate of ice. In order to generate a better cirrus cloud parameterization, we must have a better understanding of cloud formation and maintenance under different atmospheric conditions.

The purpose of this study is to do a numerical investigation on the evolution and maintenance of cirrus and the interactions among cloud dynamics, microphysics, and radiation. One-dimensional models (Jensen et al. 1994; Chen et al. 1997) suffer from their simplicity in the dynamics. In those models, the vertical velocity has to be prescribed. The effect of radiative flux convergence (radiative heating rate) on the evolution of the cloud cannot be modeled. However, computationally, these 1D models can afford very detailed microphysics modules to simulate the evolution of cloud particles within the clouds. Since our main purpose is to investigate the dynamic–microphysical–radiative interactions in cirrus, it is crucial to use a two-dimensional or three-dimensional model with interactive physical links to the atmospheric conditions, cloud physics, and radiation. Therefore, we have developed a numerical model that includes three modular components: dynamic, microphysical, and radiative. Although such a model could be either 2D or 3D, we use the 2D version of the model in this study, due to limited computational resources. The model is described in the next section.

Numerical experiments presented in a companion paper (Liu et al. 2003, hereafter Part II) are designed to simulate the evolution of cirrus under different atmospheric conditions embodied in four contrasting atmospheric profiles made available by the Global Energy and Water Cycle Experiment (GEWEX) Cloud System Study (GCSS) Cirrus Cloud System Working Group (WG2). The differences among these four profiles reside in the temperature (cloud height) and static stability, allowing us to study how the evolution of cirrus responds to the thermodynamic structure of the atmosphere. Following the description of the model, the re-

sults of the simulations are presented and evaluated. In addition, several sensitivity studies designed to investigate effects of radiation, ice crystal habit, latent heating, and ice crystal ventilation on cloud evolution are also presented in Part II.

2. Model description

a. Dynamic module

In the dynamic component of the cirrus model, a set of equations is developed for describing shallow moist convective systems suitable for cirrus clouds. Although a scale analysis shows that the full continuity equation for dry air can be well approximated by the incompressible form, this is not used in our model. Instead, we apply the quasi-compressible approximation as described in Anderson et al. (1985). This is because the incompressible form of the continuity equation requires that we solve a Poisson equation (elliptic partial differential equation) for pressure. A common method of solving the Poisson equation is the relaxation method, which is iterative and thus computationally expensive. In contrast, the quasi-compressible approximation, replaces the Poisson equation with a straightforward predictive pressure change equation. This admits sound waves, limiting the size of the numerical time step, but this problem is mitigated by artificially reducing the sound wave phase speed so that a larger time step can be used. Turbulence is parameterized by approximating the eddy flux terms using a 1.5-order closure scheme (Klemp et al. 1978; Redelsperger and Sommeria 1986). The basic equations construct the dynamic framework of this cirrus model is listed in the next section.

1) THE BASIC EQUATIONS

The basic (dependent) variables in the model are horizontal velocity u , vertical velocity w , subgrid-scale turbulent kinetic energy e , potential temperature θ , air pressure p , water vapor mixing ratio q_w , and the mixing ratio q_x and number concentration N_x of each hydrometeor class. The basic equations that govern variables other than subgrid-scale turbulent kinetic energy (TKE) e will be discussed in this section, and the TKE budget equations will be discussed in detail in the next section.

In this model, each dependent variable ϕ is decomposed into three parts as

$$\begin{aligned} \phi(x, z, t) &= \phi_0(z) + \overline{\phi'(x, z, t)} + \phi''(x, z, t) \\ &= \overline{\phi(x, z, t)} + \phi''(x, z, t), \end{aligned} \quad (1)$$

where $\phi_0(z)$ is the prescribed horizontally uniform background base state, $\overline{\phi'(x, z, t)}$ represents the departure from the background base state (grid-resolvable eddy), and $\phi''(x, z, t)$ represents the subgrid-scale perturbation (grid-unresolvable eddy). Each model variable ϕ can also be separated into a grid-resolvable $\overline{\phi(x, z, t)}$ and grid-unresolvable component $\phi''(x, z, t)$. This decom-

position is done because we are unable to resolve all scales of motion in the atmosphere on the model grid. This study uses the time-dependent, nonhydrostatic primitive equations for motion, thermodynamic energy, and mass continuity of dry air, hydrometeors, and water vapor. Since cirrus clouds are shallow convective systems, appropriate scaling analysis can be done to simplify the system of equations. The Reynolds averaging technique is applied to each of the scaled equations to yield the spatially filtered properties of each variable because we have separated each variable into grid-resolvable and subgrid parts using Eq. (1). The continuity equation of dry air is treated specially by casting it into quasi-compressible form. The quasi-compressible system is computationally efficient and retains both the accuracy and the simple boundary conditions of the fully compressible system. In this kind of approach, dimensional pressure and potential temperature are the prognostic thermodynamic variables, while temperature and density are diagnosed.

The explicit forms of these equations are now summarized below in Einstein summation notation. For the equations of motion,

$$\begin{aligned} \frac{\partial \bar{u}_i}{\partial t} = & \underbrace{-\bar{u}_j \frac{\partial \bar{u}_i}{\partial x_j}}_{\text{advection}} - \underbrace{\frac{\partial}{\partial x_j} (\overline{u_j'' u_i''})}_{\substack{\text{divergence} \\ \text{of turbulent} \\ \text{momentum flux}}} - \underbrace{\frac{1}{\rho_o} \left(\frac{\partial \bar{P}'}{\partial x_i} \right)}_{\substack{\text{pressure} \\ \text{gradient} \\ \text{force}}} \\ & + \underbrace{g \delta_{i3} \left(\frac{\bar{\theta}'}{\theta_o} + 0.608 \bar{q}_v' - \bar{q}_x' - \frac{C_v \bar{P}'}{C_p P_o} \right)}_{\text{buoyancy}}, \quad (2) \end{aligned}$$

where g is the gravitational acceleration, ρ_o is the base-state density of air, C_v is the specific heat at constant volume, C_p is the specific heat at constant pressure, and δ is the delta function ($\delta_{ij} = 1$ for $i = j$ and $\delta_{ij} = 0$ for $i \neq j$). The thermodynamic variables (virtual potential temperature and pressure) are linearized in the buoyancy term while the Boussinesq approximation, which states that variations in density can be ignored except when multiplied by gravity, is also applied. We further assume that each turbulent momentum component u_j'' behaves incompressibly ($\partial u_j'' / \partial x_j = 0$), an assumption that also applies to the other equations that follow.

The pressure tendency equation, derived and approximated from the full continuity equation using the equation of state (Klemp and Wilhelmson 1978), is written as

$$\frac{\partial \bar{P}'}{\partial t} + C_s^2 (\nabla \cdot \rho_o \bar{u}_i') = 0, \quad (3)$$

where C_s is the pseudo-sound speed. The choice of C_s is not arbitrary. It must be small enough to allow a larger time step than in a fully compressible system, yet sufficiently large so that this pseudo-sound mode will not contaminate any significant meteorological signal. Anderson et al. (1985) demonstrated that with C_s greater

than twice the maximum wind speed, the quasi-compressible system produces minimal errors. Droegemeier and Wilhelmson (1987), comparing the results of numerical thunderstorm outflow simulations calculated from the quasi-compressible and fully compressible systems, showed that choosing $C_s = 100 \text{ m s}^{-1}$ produces the best result. This is the value of C_s used in our model.

The predictive equation for potential temperature θ , a conserved quantity for dry adiabatic processes, is given by

$$\frac{\partial \bar{\theta}}{\partial t} = \underbrace{-\bar{u}_j \frac{\partial \bar{\theta}}{\partial x_j}}_{\text{advection}} - \underbrace{\frac{\partial}{\partial x_j} (\overline{u_j'' \theta''})}_{\substack{\text{divergence} \\ \text{of turbulent} \\ \text{heat flux}}} + \underbrace{\left(\frac{P_{oo}}{P} \right)^{R/C_p} (Q_R + Q_C)}_{\text{adiabatic heating}}, \quad (4)$$

where C_p is the specific heat at constant pressure, R is the specific gas constant for dry air, and P_{oo} is a reference pressure often taken to be 1000 mb, while Q_R and Q_C are the heating rates due to net radiative flux convergence and phase change, respectively.

The water vapor budget equation and the conservation equations of hydrometeor mixing ratio and number concentration are given, respectively, by

$$\frac{\partial \bar{q}_v}{\partial t} = \underbrace{-\bar{u}_j \frac{\partial \bar{q}_v}{\partial x_j}}_{\text{advection}} - \underbrace{\frac{\partial}{\partial x_j} (\overline{u_j'' q_v''})}_{\substack{\text{divergence} \\ \text{of turbulent} \\ \text{water vapor flux}}} + S_v, \quad (5)$$

$$\begin{aligned} \frac{\partial \bar{q}_x}{\partial t} = & \underbrace{-\bar{u}_j \frac{\partial \bar{q}_x}{\partial x_j}}_{\text{advection}} - \underbrace{\frac{\partial}{\partial x_j} (\overline{u_j'' q_x''})}_{\substack{\text{divergence} \\ \text{of turbulent} \\ \text{ice mixing} \\ \text{ratio flux}}} + \underbrace{\frac{\partial}{\partial x_3} (\overline{V_{t,x} q_x})}_{\text{gravitational fallout}} \\ & + \underbrace{S_{q_x, \text{diff}} + S_{q_x, \text{coll}} + S_{q_x, \text{nuc}}}_{\substack{\text{sources/sinks due to} \\ \text{microphysical processes}}}, \quad (6) \end{aligned}$$

$$\begin{aligned} \frac{\partial \bar{N}_x}{\partial t} = & \underbrace{-\bar{u}_j \frac{\partial \bar{N}_x}{\partial x_j}}_{\text{advection}} - \underbrace{\frac{\partial}{\partial x_j} (\overline{u_j'' N_x''})}_{\substack{\text{divergent} \\ \text{of turbulent} \\ \text{ice number} \\ \text{concentration} \\ \text{flux}}} + \underbrace{\frac{\partial}{\partial x_3} (\overline{V_{t,x} N_x})}_{\text{gravitational fallout}} \\ & + \underbrace{S_{N_x, \text{diff}} + S_{N_x, \text{coll}} + S_{N_x, \text{nuc}}}_{\substack{\text{sources/sinks due to} \\ \text{microphysical processes}}}. \quad (7) \end{aligned}$$

The last term in the water vapor budget equation (S_v) represents the mass transfer between the vapor phase and hydrometeors; $V_{t,x}$ in Eqs. (6)–(7) is the terminal velocity of the hydrometeor class x . The microphysical sources and sinks of the hydrometeor number concentration and mixing ratio are due to diffusional growth

($S_{N_x, \text{diff}}$, $S_{q_x, \text{diff}}$), collection processes ($S_{N_x, \text{coll}}$, $S_{q_x, \text{coll}}$), and nucleation mechanisms ($S_{N_x, \text{nuc}}$, $S_{q_x, \text{nuc}}$), respectively. These terms link the dynamic module and the other two modules.

2) TURBULENCE CLOSURE SCHEME

Due to the presence of turbulent flux terms (subgrid eddy transports) resulting from Reynolds averaging, the number of unknowns is larger than the number of equations given in the previous section. In order to close this set of equations, turbulent fluxes have to be approximated in terms of known quantities. The parameterization of subgrid eddies in our model is the 1.5-order turbulent closure scheme used by Klemp and Wilhelmson (1978) and Redelsperger and Sommeria (1986). This is sometimes referred to as local closure; that is, an unknown quantity at any point in space is parameterized in terms of values and gradients of known quantities at the same point. Local closure thus assumes that turbulence is analogous to molecular diffusion. In this type of approach, a prognostic equation for turbulent kinetic energy e is specified, and the values of e calculated from this equation are then used to diagnose eddy mixing coefficients for momentum, heat, and moisture.

The subgrid-scale turbulent kinetic energy is defined as

$$e = \frac{1}{2} \overline{(u''_i)^2}. \quad (8)$$

Thus, following the derivation of the budget equation as in Stull (1988), the TKE budget equation can be written as

$$\begin{aligned} \frac{\partial \bar{e}}{\partial t} + \overline{u_i} \frac{\partial \bar{e}}{\partial x_j} &= \delta_{is} g \left(\frac{\overline{u_i'' \theta_v''}}{\theta_v} - \overline{u_i'' q_T''} \right) - \overline{u_i'' u_j''} \frac{\partial \bar{u}_i}{\partial x_j} - \nu \left(\frac{\partial \bar{u}_i''}{\partial x_j} \right)^2, \quad (9) \\ \text{A} \quad \text{B} & \quad \text{C} \quad \text{D} \quad \text{E} \end{aligned}$$

where ν is the molecular viscosity of air and q_T the total water mixing ratio (all phases). The terms A and B on the left-hand side of (9) represent the respective local storage of TKE and the advection of TKE by the grid-resolvable wind. Term C is the buoyant production or consumption of TKE. Term D is the mechanical or shear-generated production/loss of TKE, and the last term E represents the viscous dissipation of TKE.

The dissipation term E is approximated as

$$-\nu \left(\frac{\partial \bar{u}_i''}{\partial x} \right)^2 = - \left(\frac{C_m \bar{e}^{1.5}}{L} \right), \quad (10)$$

where $C_m = 0.2$ (Deardorff 1972). We approximate the mixing length L as usual by relating it to the model grid dimensions:

$$L = (\Delta x \Delta z)^{1/2}, \quad (11)$$

where Δx and Δz are the grid spacings. The eddy flux of momentum, in term D of (9) and in the equation of motion (2), can be parameterized as

$$\overline{(u_i'' u_j'')} = -K_m \left(\frac{\partial \bar{u}_i}{\partial x_j} + \frac{\partial \bar{u}_j}{\partial x_i} \right) + \frac{2}{3} \delta_{ij} \bar{e}. \quad (12)$$

Here, K_m is the eddy mixing coefficient for momentum and is related to the turbulent kinetic energy by

$$K_m = C_m L \bar{e}^{0.5}. \quad (13)$$

The eddy moisture and heat fluxes in the respective moisture conservation and thermodynamic equations are defined as

$$\overline{(u_i'' \phi'')} = -K_h \frac{\partial \bar{\phi}}{\partial x_i}, \quad (14)$$

where $K_h = 3K_m$ is the eddy mixing coefficient for heat and moisture. The factor 3 is based on Deardorff's results (1972) from numerical simulations of unstable and neutral planetary boundary layers. Eddy mixing coefficients for hydrometeors are assumed identical to K_h .

The buoyancy term C in the equation for the generation of TKE in saturated conditions can be approximated by

$$\begin{aligned} \left(\frac{\overline{u_i'' \theta_v''}}{\theta_v} - \overline{u_i'' q_T''} \right) &= \left(\frac{BK_h}{\theta_v} \right) \left(\frac{\partial \bar{\theta}_{ei}}{\partial x_i} - \frac{L_{vi} P_o}{C_p T_o} \frac{\partial \bar{q}_i}{\partial x_i} \right) + K_h \frac{\partial \bar{q}_T}{\partial x_i}, \quad (15) \end{aligned}$$

where θ_{ei} is an equivalent potential temperature, which takes ice processes into account, while T_o and P_o are the respective base state temperature and pressure; B is written as

$$B = \frac{1 + 0.61 \frac{\varepsilon L_{vl} q_v}{R_d T}}{1 + \frac{\varepsilon L_{vl}^2 q_v}{C_p R_d T^2}}, \quad \varepsilon = 0.622; \quad (16)$$

and L_{vl} and L_{vi} are the latent heat of condensation and sublimation, respectively. The buoyancy term for unsaturated conditions can be written as

$$\left(\frac{\overline{u_i'' \theta_v''}}{\theta_v} - \overline{u_i'' q_T''} \right) = - \left(\frac{K_h}{\theta_v} \right) \frac{\partial \bar{\theta}}{\partial x_i}. \quad (17)$$

At this point, the turbulent kinetic energy is closed and the value of e is obtained, so that eddy mixing coefficients can then be calculated.

In order to close the turbulent flux terms in the prognostic equations for momentum, heat, moisture, and hydrometeors, those terms are parameterized in the same fashion as in Eqs. (12) and (14).

TABLE 1. Power-law relationships for ice crystals (cgs unit). Width is denoted as W , diameter is D , and length is L .

Habit	Dimensional relationship	Projected area (A)-dimensional relationship	Mass (m)-dimensional relationship	Capacitance (C)-dimensional relationship
Spheres	$W = D$	$A = \frac{\pi}{4}D^2$	$m = \rho_i \frac{\pi}{6}D^3$	$C = 0.5D$
Plates	$W = 0.0141D^{0.475}$	$A = 0.2395D^{1.855}$	$m = 0.007384D^{2.449}$	$C = 0.277D^{0.99}$
Columns	$D = 0.26L^{0.927}$	$A = 0.0459L^{1.415}$	$m = 0.01658L^{1.91}$	$C = 0.278D^{0.97}$
Rosettes	$W = D$	$A = 0.0869D^{1.57}$	$m = 0.0459D^{1.415}$	$C = 0.5D$
Aggregates	$W = D$	$A = 0.2285D^{1.88}$	$m = 0.00281D^{0.21}$	$C = 0.5D$

3) NUMERICAL METHODS, GRID SETUP, AND BOUNDARY CONDITIONS

The time splitting integration technique proposed by Klemp and Wilhelmson (1978) is included. The integration process is split into two parts: one is for non-sound-wave-related variables using a larger time step, the other is for sound-wave-related variables using a smaller time step. The time integration is done with second-order centered differences. Subgrid-scale turbulent kinetic energy, water vapor, and potential temperature are numerically advected using the sixth-order Crowley scheme (see Tremback et al. 1987), while hydrometeors are advected using a total variation diminishing (TVD) scheme (Yee 1987). The TVD scheme is introduced here because most numerical advection schemes are dispersive across the discontinuity (the interface between the environment and an advected disturbance), and thus may lead to unphysical negative values across a discontinuity for positive definite variables such as mixing ratios (or concentrations) of hydrometeors. Therefore, the TVD scheme is applied to the advection of hydrometeors, because this scheme can effectively eliminate the artificial oscillation across the discontinuity.

The Arakawa C grid (Arakawa and Lamb 1981) is used in this model. It is a staggered grid system in which velocity components and scalar variables are located at the respective normal faces and centers of grid cells. This staggered grid system is found to be more computationally stable than an unstaggered one. The grid spacings in the horizontal and vertical directions are set to 200 and 100 m, respectively.

The boundary conditions are chosen similar to Starr and Cox (1985). Free slip condition is imposed on the horizontal component of velocity variable ($\partial u/\partial z = 0$) at the upper and lower boundaries, where the eddy diffusion terms are also specified as zero, whereas hydrometeors are allowed to fall across the lower boundary. The perturbation vertical wind and the perturbation pressure are assumed to cease at upper and lower boundaries. This is to say that vertical wind and pressure are kept at their basic-state values along top and bottom boundaries. The advection term for a scalar variable at the upper and lower boundaries is setup as the gradient of the advection term is zero. Along the boundaries, we presently set the normal mixing term equal to zero. This approach ensures that vertical gradients in the mean state

profiles are not distorted due to eddy mixing near the boundaries. Cyclic boundary conditions are applied in the horizontal direction. The impinging of updrafts and downdrafts on stable atmosphere above and below the cloud deck generates gravity waves. Rigid boundary conditions reflect the waves back to the domain and cause false interaction of these waves with the cloud. Thus, artificial sponge layers are added to the lower and upper parts of the domain to absorb the energy of a wave and to reduce wave reflection. We use a so-called Rayleigh damping proposed by Klemp and Lilly (1978) in the absorbing layer. In the absorbing layer, only the perturbations of a variable from its upstream values are damped.

b. Microphysics module

A double-moment microphysical parameterization, as proposed by Ferrier (1994), is used to describe the evolution of the hydrometeor size distribution. This method assumes that various ice categories may be represented by the given specified size distribution functions. Parameterizations are then developed for various physical processes including nucleation, diffusional growth, and collisional growth of ice crystals, transferring mass between the various hydrometeor classes based on the assumed size distributions. Both the mixing ratio and number concentration of ice crystals are predicted at each grid location. The mean ice crystal diameter can then be diagnosed from these two quantities. Thus, the evolution of ice crystal size spectra can be more realistically resolved.

In this cirrus model, hydrometeors are categorized into two forms: pristine ice crystals and ice crystal aggregates. The mathematical form used here to parameterize the size spectrum of ice crystals is the inverse exponential gamma distribution. According to observational data, many ice crystal characteristics such as mass, projected area, and dimension can be approximated as powers of the characteristic length (e.g., Auer and Veal 1970). The power laws used in this model are summarized in Table 1.

It has been shown by Starr and Cox (1985) that the evolution of cirrus is highly sensitive to the terminal velocity of ice crystal because the terminal velocity controls the sedimentation rate of cirrus and thus affects its vertical extent and optical depth. Therefore, in order to

simulate the ice crystal fallout effect more realistically, we adopted a method as described in Johnson (1997) in which he combined the work of Böhm (1989) and Mitchell (1996) to formulate the ice crystal terminal velocity with a power-law relationship with ice crystal diameter. The coefficients of this power law are not constant; instead, these coefficients are functions of ambient air properties, coefficients of other power-law relationships for ice such as mass-dimensional and projected area-dimensional relationships, and also a power-law relationship for the Reynolds–Best number proposed by Mitchell (1996). Unlike empirical terminal velocity formulas that are fitted to specific datasets, Johnson’s approach provides a unified terminal velocity parameterization for all ice habits. It does not represent particles as spheroids, but is general for any particle shape and size. It is conceptually and mathematically simple, appears accurate, and provides for physical insight.

Heterogeneous and homogeneous freezing nucleation mechanisms are considered in our model. A simple function of ice supersaturation is used for the deposition and condensation-freezing modes of heterogeneous nucleation, as proposed by Meyers et al. (1992). Although Meyers’ function has been widely used, it should be noted that the formulation is based on measurements made at the earth’s surface over a limited temperature range. Here, in this study, we extrapolate the temperature-dependent formula to all the possible temperature ranges for cirrus cloud. The impact of doing so is unknown and data are scarce to validate the values of heterogeneous ice nucleation concentrations predicted at low temperatures. For homogeneous nucleation processes, we use the parameterization proposed by DeMott et al. (1994) to estimate the homogeneous freezing nucleation rates, while assuming the cloud condensation nuclei (CCN) consist of ammonium sulfate aerosols.

The rate of mass growth of a single hydrometeor by vapor deposition can be approximated as

$$\frac{dm}{dt} = 4\pi CG(T, P)(S - 1), \quad (18)$$

where $G(T, P)$ is the thermodynamic function

$$\frac{1}{G(T, P)} = \frac{L^2}{KR_v T^2} + \frac{R_v T}{D_v e_{\text{sat}}} \quad (19)$$

and e_{sat} is the saturation vapor pressure, D_v is the vapor diffusivity coefficient, R_v the moist gas constant, L is the latent heat associated with the process, and C the capacitance of the hydrometeor. In the diffusional growth equation of an ice crystal, both capacitance and ventilation coefficients are functions of ice crystal shape. Therefore, several new treatments for capacitance and ventilation coefficients (Ji and Wang 1999), crucial determinants of ice crystal growth, are considered in this model study. We also assume perfect mass accommodation whenever water vapor lands on the ice surface.

TABLE 2. Ice crystal capacitance. Semimajor axis length is denoted by a , semiminor axis length is b , and diameter of a sphere is D .

	Expression	Sources
Columns	Approximated by charged circular cylinders $C = \left[0.708 + 0.615 \left(\frac{b}{a} \right)^{0.76} \right] a$	Smythe (1956, 1962); Wang et al. (1985)
Plates	Approximated by oblate spheroids $C = \frac{a\varepsilon}{\sin^{-1}\varepsilon} \quad \varepsilon = \left(1 - \frac{b^2}{a^2} \right)^{0.5}$	Pruppacher and Klett (1978)
Sphere rosettes	$C = \frac{1}{2}D$	

The ice crystal capacitance, obtained by electrostatic analogy, has dimensions of length and is a function of particle size and shape. In this study, the capacitance of a platelike ice crystal is approximated by that of an oblate spheroid, while bullet rosettes are treated as spheres. Both McDonald (1963) and Heymsfield (1975) pointed out that the capacitance of particles with more protruding spatial branches, such as rosettes, could be approximated by that for spherical particles. Wang et al. (1985) have shown that using the capacitance of prolate spheroids for columns, in calculating the vapor density fields surrounding stationary columnar ice crystals, is inadequate. Therefore, as an alternative for columnar crystals, C has been defined by analogy to the capacitance of charged right circular cylinders (Smythe 1956, 1962; Wang et al. 1985; Johnson 1997). The capacitances for three ice crystal types are summarized in Table 2. To assist in the integration of the diffusional growth equation, the capacitance is written as a power-law approximation:

$$C = c_c D^{p_c}. \quad (20)$$

The coefficients and the powers for Eq. (20) are listed in Table 1. For a given crystal diameter, the sphere/rosette has the largest capacitance; the column, second largest; and the plate, the smallest among the three crystal types.

When particles are large enough to have appreciable terminal velocities, the vapor density gradient is increased ahead of the particles, as are the rates of heat and mass transfer. The effect of this ventilation on the vapor deposition rate is represented by multiplying the depositional growth equation by a ventilation coefficient f_v , defined as

$$\left. \frac{dm}{dt} \right|_{vd} = f_v \left(\left. \frac{dm}{dt} \right|_{vd/0} \right), \quad (21)$$

where the subscript 0 indicates the depositional mass growth of a stationary particle.

For spherical ice hydrometeors, the ventilation coefficient is taken from Hall and Pruppacher (1976), who gave the following expressions:

TABLE 3. Ventilation coefficients for ice crystals.

Habit	C_1	C_2
Columns	0.0309	0.1447
Plates	0.0105	0.0228
Bullet rosettes	0.3005	-0.0022

$$f_v = \begin{cases} 1.0 + 0.14X^2 & X < 1.0 \\ 0.86 + 0.28X & X \geq 1.0, \end{cases} \quad (22)$$

where

$$X = Sc^{1/3}Re^{1/2}$$

and Sc is the Schmidt number, while Re is the Reynolds number.

For nonspherical ice particles such as columns and plates, the ventilation coefficients are represented by a second-order polynomial (Johnson 1997) that is based on the results of Ji and Wang (1999):

$$f_v = 1.0 + C_1X + C_2X^2. \quad (23)$$

The coefficients C_1 and C_2 for columns and plates are shown in Table 3. For bullet rosettes, the ventilation coefficient is based on Jayaweera (1971) and Heymsfield (1975):

$$f = 1 + \frac{2(L + D)}{4\pi C} (0.6) \left[\frac{\frac{\pi D}{4} + \pi L}{2(L + D)} \right]^{1/2} Re_d^{1/2}, \quad (24)$$

where $Re_d = (V_t D)/\nu$ is the Reynolds number, V_t is the terminal velocity, D is the bullet diameter, L is the bullet length, and C is the capacitance. In order to express the ventilation coefficient for rosettes as a function of Schmidt and Reynolds numbers Eq. (22) was approximated by Eq. (21) with coefficients as listed in Table 3. The ventilation coefficients for all ice crystals are shown in Fig. 1 as a function of Schmidt and Reynolds numbers. In general, the ventilation coefficient for ice crystal varies significantly with crystal shape, leading to different mass diffusion rates for different crystal type. For a given crystal diameter, columns have the greatest ventilation effect, while the plates have the smallest effect. The ventilation effect of ice spheres and rosettes are similar to each other, and intermediate between those of columns and plates. However, bullet rosettes have slightly greater ventilation than spheres.

Ice particles collide with each other when their terminal velocities differ and their concentrations are large enough so that one hydrometeor type sweeps out a population of another species. The transfer of mass from one hydrometeor to another, however, also depends on whether coalescence occurs. That, in turn, depends on the hydrometeor type and mass, as well as environmental conditions. Hydrometeors of the same type can also collide and coalesce (self-collection process) with each other and become a larger particle. Thus, the self-collection process can contribute to a mass transfer from

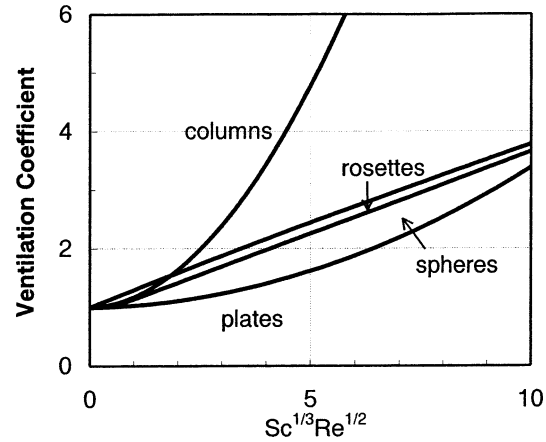


FIG. 1. Ventilation coefficients for columns, plates, bullet rosettes, and spheres.

a pristine ice category to an aggregates category. In order to calculate the ice aggregation processes between different ice categories and within the same category (self-collection), the formulations proposed by Verlinde et al. (1990) are utilized in our model. The coalescence efficiency is assumed to be 1, and the collision efficiency is set to 0.1 (Kajikawa and Heymsfield 1989).

c. Radiation module

In order to calculate the radiative heating rates at each grid point, the radiative transfer equations have to be specified and the cloud optical properties determined. Since the upward and downward fluxes in a given atmospheric layer are the main concern here, it is not necessary to calculate the radiance distribution at each level. Instead, a two-stream/adding model (Ackerman and Stephens 1987) is used to calculate radiative fluxes at each grid point. The one applied here is a narrowband model, which divides the solar and terrestrial radiation spectra into 11 and 20 bands, respectively.

The cirrus cloud deck is usually optically thin and the mean free path for a photon colliding with a particle in cirrus is much larger than that in a typically stratocumulus cloud deck. Therefore, the radiative heating is distributed through the entire cirrus cloud body instead of being distributed like two Dirac functions with opposite signs at the cloud top and bottom as in a typical stratocumulus cloud (Ackerman et al. 1988). Moreover, the volume absorption coefficient and the volume extinction coefficient are very sensitive to the ice crystal size distribution. As the cloud evolves, the change in ice crystal size distribution causes changes in the radiative heating rates not only in the interior but also below and above the cloud deck. It is therefore important to correctly represent the ice crystal optical properties. The anomalous diffraction theory (ADT) was originally proposed by van de Hulst (1981) as an approximation of Mie theory to calculate the optical prop-

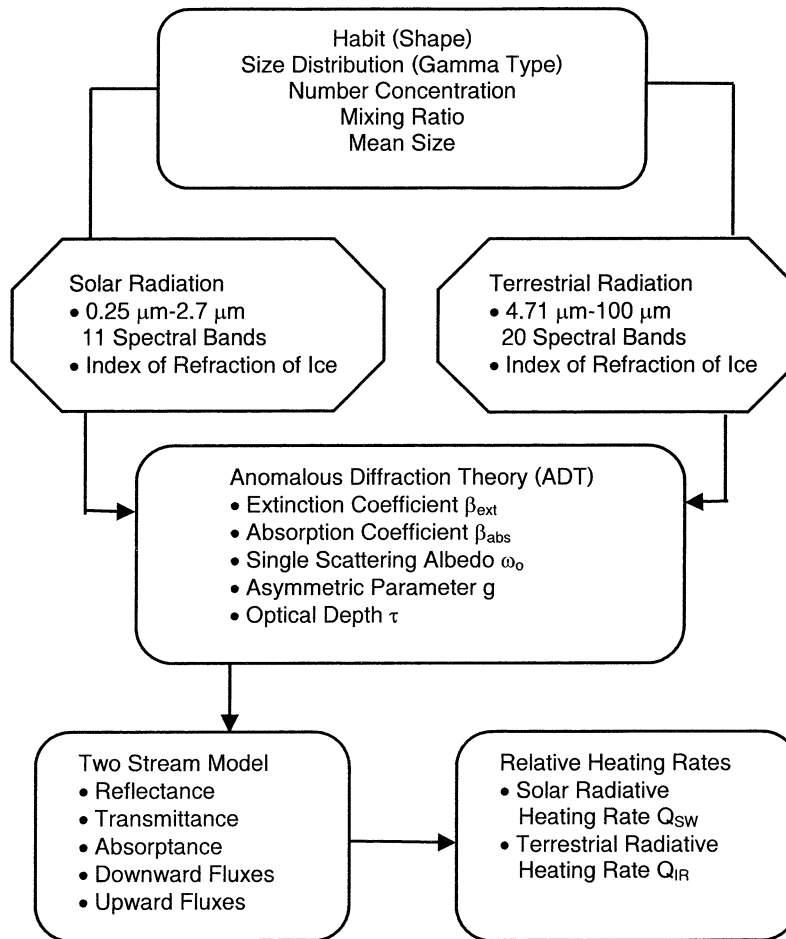


FIG. 2. Links between the microphysics module and the radiation module.

erties of spherical particles. The original ADT captures the fundamental behavior of Mie theory, including the phase of the interference patterns apparent in extinction efficiencies. However, it predicts that the incident radiation passes directly through a particle without refracting or experiencing internal reflections, and does not account for tunneling processes. Ackerman and Stephens (1987) expanded the original ADT to approximate the radiative properties of water clouds by parameterizing edge effects for the extinction efficiencies and refraction effects for the absorption efficiencies. Inclusion of the refractive effects lengthens the ray path through the particle, thus enhancing the predicted absorption and improving the overall performance of ADT. Mitchell (2000) reformulated the anomalous diffraction theory in terms of a particles' effective photon path, and modified to reproduce Mie theory within 10% for water and ice spheres regarding extinction and absorption. In this reformulation of the modified anomalous diffraction theory (MADT), he parameterized the processes of internal reflection/refraction and photon tunneling to yield analytical expressions for the absorption and extinction coefficients of water drops, and expanded the applica-

tion of ADT to nonspherical particles for the internal reflection/refraction processes. The extent to which tunneling processes apply to ice particles depends on morphology, and is an active area of research. In our radiation module, we adopt Mitchell's approach to calculate the optical properties of cirrus. The advantages of Mitchell's parameterizations are that the absorption and extinction coefficients are analytical functions of the size distribution parameters, shapes (or habits), wavelengths, and refractive index. Therefore, the optical properties calculated are explicit functions of ice crystal geometry and are not based on an effective radius that has little physical meaning. Another advantage of MADT is that the scattering properties in the thermal infrared spectral range can be explicitly calculated, so that the scattering is not ignored.

The links between the radiative transfer and microphysics modules to calculate the radiative heating rates are illustrated in Fig. 2. The absorption, extinction, and single scattering albedo can be calculated accurately for both the solar and terrestrial spectra, and scattering is not ignored when calculating thermal infrared radiation. In this study, the radiative heating rates are calculated

separately for solar and terrestrial spectra. Vertical atmospheric columns are assumed independent of each other. Consequently, interactions of radiative flux among adjacent columns are ignored. The indices of refraction for ice in this study are from Warren (1984).

3. Summary

A two-dimensional quasi-compressible numerical cloud model is developed to simulate the evolution of cirrus. The model contains three modules embodying dynamics, microphysics, and radiation, along with heterogeneous and homogeneous nucleation of haze particles. In the dynamics module, a set of equations is developed for a shallow moist convective system. Advection terms in the particle transport equations are calculated using the TVD scheme to ensure preservation of positive definiteness for microphysical variables such as ice mixing ratio and number concentration. The TVD scheme not only ensures the positive definiteness of the microphysical variables (mixing ratio and number concentration) being advected, but also reduces computational errors resulting from numerical dispersions. Sub-grid eddy transports are parameterized using a 1.5-order turbulence closure scheme. The main feature of the microphysics module is a double-moment scheme to simulate the evolution of the ice crystal size distributions. Diffusional growth, sedimentation, and aggregation of ice crystals are explicitly calculated. Heterogeneous and homogeneous nucleation of haze particles are included. Ventilation coefficients for different habits of ice crystals are used, based upon calculations of the flow field around a single ice crystal falling at its terminal velocity as well as upon solving the convection–diffusion equation for the water vapor density field around the moving ice crystals. In the radiation module, a two-stream radiative transfer model is used to calculate the radiative fluxes and heating rates, while the cloud optical properties are obtained by the modified anomalous diffraction theory for both spherical and nonspherical particles. Scattering by ice crystals accounted for in the model infrared heating rate, since the extinction properties for thermal infrared radiation can be calculated accurately by modified anomalous diffraction theory. Unlike most of the existing parameterizations for ice crystal optical properties that are derived from limited sets of observations or laboratory results, MADT has more physics behind the parameterization. The major advantage of this cirrus model is that both microphysical and radiative properties are calculated as explicit functions of ice crystal habit. Thus, sensitivity of the cloud evolution to ice crystal habit can be investigated.

The focus of this study, the evolution of cirrus clouds, is embodied in four simulation sets to be presented in Part II. The first simulation set is designed to investigate the sensitivity of cirrus evolution to the environmental temperature (warm versus cold) and static stability (stable versus unstable). As will be seen in Part II, the results

suggest that cirrus cloud development is very sensitive to both these parameters and indicate that homogeneous nucleation and cold temperatures are the two major factors that favor persistent cirrus clouds. The other simulation sets to be presented in Part II are designed to study the effects of radiative processes, latent heat, ice crystal habit, and ice aggregation on cirrus evolution, respectively.

Acknowledgments. This research is partially supported by NSF Grants ATM-9314465, 9633424, 9714158, 9907761, and 0234744. One of us (PKW) would like to thank the Alexander von Humboldt Foundation of Germany for the Humboldt Award that supported his research visit to the University of Mainz, Germany, in 1993.

REFERENCES

- Ackerman, S. A., and G. L. Stephens, 1987: The absorption of solar radiation by cloud droplets: An application of anomalous diffraction theory. *J. Atmos. Sci.*, **44**, 1574–1588.
- Ackerman, T. P., N. K. Liou, F. P. J. Valero, and L. Pfister, 1988: Heating rates in tropical anvils. *J. Atmos. Sci.*, **45**, 1606–1623.
- Anderson, J. K., K. Droegemier, and R. B. Wilhelmson, 1985: Simulation of the thunderstorm subcloud environment. Preprints, *14th Conf. on Severe Local Storms*, Indianapolis, IN, Amer. Meteor. Soc., 147–150.
- Arakawa, A., and V. R. Lamb, 1981: A potential enstrophy conserving scheme for the shallow water equations. *Mon. Wea. Rev.*, **109**, 18–36.
- Auer, A. H., and D. Veal, 1970: The dimensions of ice crystals in natural clouds. *J. Atmos. Sci.*, **27**, 919–926.
- Böhm, J. P., 1989: A general equation for the terminal fall speed of solid hydrometeors. *J. Atmos. Sci.*, **46**, 2419–2427.
- Chen, J. P., G. M. McFarquhar, and A. J. Heymsfield, 1997: A modeling and observational study of the detailed microphysical structure of tropical cirrus anvil. *J. Geophys. Res.*, **102**, 6637–6653.
- Deardorff, J. W., 1972: Numerical investigation of neutral and unstable planetary boundary layers. *J. Atmos. Sci.*, **29**, 91–115.
- Del Genio, A. D., M. S. Yao, W. Kovari, and K. K. W. Lo, 1996: A prognostic cloud water parameterization for global climate models. *J. Climate*, **9**, 270–304.
- DeMott, P. J., M. P. Meyers, and W. R. Cotton, 1994: Numerical model simulations of cirrus clouds including homogeneous and heterogeneous ice nucleation. *J. Atmos. Sci.*, **51**, 77–90.
- Droegemeier, K. K., and R. B. Wilhelmson, 1987: Numerical simulation of thunderstorm outflow dynamics. Part I: Outflow sensitivity experiments and turbulence dynamics. *J. Atmos. Sci.*, **44**, 1180–1210.
- Ferrier, B. S., 1994: A double scheme multiple-phase four-class bulk ice scheme. Part I. Description. *J. Atmos. Sci.*, **51**, 249–280.
- Fowler, L. D., D. A. Randall, and S. A. Rutledge, 1996: Liquid and ice cloud microphysics in the CSU general circulation model. Part I. Model description and simulated microphysical processes. *J. Climate*, **9**, 489–529.
- Hall, W. D., and H. R. Pruppacher, 1976: The survival of ice particles falling from cirrus clouds in subsaturated air. *J. Atmos. Sci.*, **33**, 1995–2006.
- Heymsfield, A. J., 1975: Cirrus uncinus generating cells and the evolution of cirroform clouds. Part III. *J. Atmos. Sci.*, **32**, 799–808.
- Jayaweera, K. O. L. F., 1971: Calculations of ice crystal growth. *J. Atmos. Sci.*, **28**, 728–736.
- Jensen, E. J., O. B. Toon, D. L. Westphal, S. Kinne, and A. J. Heymsfield, 1994: Microphysical modeling of cirrus. 1. Comparison with 1986 FIRE IFO measurements. *J. Geophys. Res.*, **99**, 10 421–10 442.

- Ji, W., and Pao K. Wang, 1999: Ventilation coefficients of falling ice crystals at low-intermediate Reynolds numbers. *J. Atmos. Sci.*, **56**, 829–836.
- Johnson, D. E., 1997: An examination of the microphysical and dynamical processes in a winter storm. Ph.D. dissertation, Dept. of Meteorology, University of Wisconsin—Madison, 347 pp.
- Kajikawa, M., and A. J. Heymsfield, 1989: Aggregation of ice crystals in cirrus. *J. Atmos. Sci.*, **46**, 3108–3121.
- Klemp, J. B., and D. K. Lilly, 1978: Numerical simulation of hydrostatic mountain waves. *J. Atmos. Sci.*, **35**, 78–107.
- , and R. B. Wilhelmson, 1978: The simulation of three-dimensional convective storm dynamics. *J. Atmos. Sci.*, **35**, 1070–1096.
- Liou, K. N., 1992: *Radiation and Cloud Processes in the Atmosphere*. Oxford University Press, 487 pp.
- Liu, H.-C., P. K. Wang, R. E. Schlesinger, 2003: A numerical study of cirrus clouds. Part II: Effects of ambient temperature, stability, radiation, ice microphysics, and microdynamics on cirrus evolution. *J. Atmos. Sci.*, **60**, 1097–1119.
- McDonald, J. E., 1963: Use of the electrostatic analogy in studies of ice crystal growth. *Z. Angew. Math. Phys.*, **14**, 610–620.
- Meyers, M. P., P. J. DeMott, and W. R. Cotton, 1992: New primary ice nucleation parameterizations in an explicit cloud model. *J. Appl. Meteor.*, **31**, 708–721.
- Mitchell, D. L., 1996: Use of mass- and area-dimensional power laws for determining precipitation particle terminal velocities. *J. Atmos. Sci.*, **53**, 1710–1723.
- , 2000: Parameterization of the Mie extinction and absorption coefficients for water clouds. *J. Atmos. Sci.*, **57**, 1311–1326.
- Pruppacher, H. R., and J. D. Klett, 1978: *Microphysics of Clouds and Precipitation*. D. Reidel, 714 pp.
- Ramanathan, V., E. J. Pitcher, R. C. Malone, and M. L. Blackmon, 1983: The response of a spectral general circulation model to refinements in radiative processes. *J. Atmos. Sci.*, **40**, 605–630.
- Ramaswamy, V., and V. Ramanathan, 1989: Solar absorption of cirrus clouds and the maintenance of the tropical upper troposphere thermal structure. *J. Atmos. Sci.*, **46**, 2293–2310.
- Randall, D. A., Harshvardan, D. A. Dazlich, and T. G. Corsetti, 1989: Interactions among radiation, convection, and large-scale dynamics in a general circulation model. *J. Atmos. Sci.*, **46**, 1943–1970.
- Redelsperger, J. L., and G. Sommeria, 1986: Three-dimensional simulation of a convective storm: Sensitivity studies on subgrid parameterization and spatial resolution. *J. Atmos. Sci.*, **43**, 2619–2635.
- Smythe, W. R., 1956: Charged right circular cylinders. *J. Appl. Phys.*, **27**, 917–920.
- , 1962: Charged right circular cylinders. *J. Appl. Phys.*, **33**, 2966–2967.
- Starr, D. O’C., and S. K. Cox, 1985: Cirrus clouds. Part I. A cirrus cloud model. *J. Atmos. Sci.*, **42**, 2663–2681.
- Stull, R. B., 1988: *An Introduction to Boundary Layer Meteorology*. Kluwer Academic, 666 pp.
- Tremback, C. J., J. Powell, W. R. Cotton, and R. A. Pielke, 1987: The forward-in-time upstream advection scheme: Extension to higher order. *Mon. Wea. Rev.*, **115**, 540–555.
- van de Hulst, H. C., 1981: *Light Scattering by Small Particles*. Dover, 470 pp.
- Verlinde, J., P. J. Flatau, and W. R. Cotton, 1990: Analytical solutions to the collection growth equation: Comparison with approximate methods and application to cloud microphysics parameterization schemes. *J. Atmos. Sci.*, **47**, 2871–2880.
- Wang, P. K., C. H. Chuang, and N. L. Miller, 1985: Electrostatic, thermal and vapor density fields surrounding stationary columnar ice crystals. *J. Atmos. Sci.*, **47**, 2371–2379.
- Warren, S. G., 1984: Optical constants of ice from ultraviolet to the microwave. *Appl. Opt.*, **23**, 1206–1225.
- Yee, H. C., 1987: Construction of explicit and implicit symmetric TVD schemes and their applications. *J. Comput. Phys.*, **68**, 151–179.